

ARTICLE

Linear flow-velocity gradient chromatography—An efficient method for increasing the process efficiency of batch and continuous capture chromatography of proteins

Chyi-Shin Chen¹  | Kosei Ando¹ | Noriko Yoshimoto^{1,2}  | Shuichi Yamamoto^{1,2} 

¹Graduate School of Science and Technology for Innovation, Yamaguchi University, Ube, Japan

²Biomedical Engineering Center (YUBEC), Yamaguchi University, Ube, Japan

Correspondence

Shuichi Yamamoto, Graduate School of Science and Technology for Innovation, Yamaguchi University, Ube 755-8611, Japan.
Email: shuichi@yamaguchi-u.ac.jp

Abstract

A new method was proposed for increasing the capture chromatography process efficiency, linear flow-velocity gradient (LFG). The method uses a linear decreasing flow-velocity gradient with time during the sample loading. The initial flow velocity, the final flow velocity and the gradient time are the parameters to be tuned. We have developed a method for determining these parameters by using the total column capacity and the total loaded amount as a function of time. The capacity can be calculated by using the relationships between dynamic binding capacity (DBC) and residence time. By leveraging the capacity, loading amount, and the required conditions, the optimum LFG can be designed. The method was verified by ion-exchange and protein A chromatography of monoclonal antibodies (mAbs). A two-fold increase in the productivity during the sample loading was possible by LFG compared with the constant flow-velocity (CF) operation. LFG was also applied to a 4-column continuous process. The simulation showed that the cost of resin per unit amount of processed mAbs can be reduced by 13% while 1.4 times enhancement in productivity was preserved after optimization by LFG compared to CF. The process efficiency improvement is more pronounced when the isotherm is highly favorable and the loading volume is large.

KEYWORDS

capture chromatography, continuous chromatography, flow velocity programming, linear flow-velocity gradient, monoclonal antibodies

1 | INTRODUCTION

Monoclonal antibodies (mAbs) are key groups in therapeutic proteins being rapidly growing in clinical practices (Ecker et al., 2015). As mAbs are the largest class, manufacturing of therapeutic mAbs with high purity and efficiency at commercial scales is required to match the market demand. Capture chromatography processes are considered as the bottleneck in the downstream process of mAbs with recent advancement in upstream processes because of its insufficient process efficiency and high-cost share in the overall manufacturing process.

To alleviate the economic overburden from process chromatography in therapeutic antibodies, new downstream process technologies are needed to integrate the manufacturing platform to drive efficacy.

The first step of the downstream process of mAbs is most commonly by protein A capture chromatography. The process performance is generally being evaluated by productivity P , which is the production rate over column volumes. The amount of product adsorbed in a chromatography column can be represented by the dynamic binding capacity (DBC), which is affected by multiple factors including resin media, feed concentration, flow rate, pH, temperature, and so forth as reported in other studies

This is an open access article under the terms of the Creative Commons Attribution-NonCommercial-NoDerivs License, which permits use and distribution in any medium, provided the original work is properly cited, the use is non-commercial and no modifications or adaptations are made.

© 2020 The Authors. *Biotechnology and Bioengineering* Published by Wiley Periodicals LLC

(Carta & Jungbauer, 2010; Fahrner et al., 1999). Although DBC increases with the residence time (RT), the total process time becomes longer, which reduces P . Therefore, RT is decreased (flow rate is increased) to increase P for the capture process. Usually, the flow rate during the sample loading is constant. However, for the capture process it was already shown that a dual-flow rate or multiple-step flow rate strategy during the sample loading can increase DBC (Becerra-Arteaga, 2016; Bjorkman, 2014; Ghose et al., 2004, 2014). The optimal flow rate profile to maximize productivity was normally determined by design of experiment (DoE) or simulation through mechanistic models of chromatography (Sellberg et al., 2018).

In this study, we propose a new method for increasing the capture chromatography process efficiency, linear flow-velocity gradient (LFG). The method uses a linear decreasing flow-velocity gradient with time during the sample loading. The initial flow velocity, the final flow velocity, and the gradient time are the parameters to be tuned. We have developed a method for determining these parameters by using the capacity of the column M_{col} and the amount of the sample loaded to the column M_{load} to make LFG much more efficient and easy-to-use compared with the step-change method. The method was verified by ion-exchange chromatography and protein A chromatography of mAb.

Regarding the recent adoption of continuous chromatography in mAb downstream processes (Baur et al., 2016; Shukla et al., 2017; Woodcock, 2014), LFG was applied to continuous processes for mAb using a 4-column periodic counter-current chromatography (PCCC) of protein A columns as an example, and the process performance was evaluated by the loading time and productivity. Comparison of the resin cost per unit mAb produced was conducted, and different conditions of LFG were discussed for the flow optimization, with advancement in both productivity and resin cost compared to the case of constant flow rate (CF) operation.

2 | THEORY

2.1 | Dynamic binding capacity

The dynamic binding capacity, DBC, is widely used for describing the actual capacity of proteins to a chromatography (packed bed) column. DBC is calculated from the breakthrough curve according to Equation (1):

$$DBC_{X\%} = \frac{C_0 V_{B,X\%}}{V_t} \quad (1)$$

Here X represents the dimensionless breakthrough curve concentration, where $X = C/C_0$. C_0 is the feed concentration, $V_{B,X\%}$ is the break through volume at $X = X\%$, and V_t is the total column (packed bed) volume. Although $DBC_{10\%}$ is commonly used for the evaluation of the resins (packed columns), $DBC_{1\%}$ was also used in the study as it is the critical value for the process chromatography. Hereafter, V_B in the study stands for $V_{B,1\%}$ unless otherwise specified.

DBC decreases with increasing mobile phase flow-velocity u or particle diameter d_p . From the mechanistic model considering the

stationary phase (pore) diffusion coefficient D_s (Carta & Jungbauer, 2010; Carta, 2012; LeVan et al., 1997), the following correlation can be derived for DBC of proteins (Chen et al., 2020):

$$E^* = \frac{DBC}{SBC} = f(F^*) = f\left(\frac{d_p^2}{D_s(Z/u)}\right) \quad (2)$$

Here SBC is the static binding capacity, which is related to the equilibrium stationary phase concentration of the chromatography resins, C_s at $C = C_0$.

The dimensionless group $F^* = d_p^2/[D_s(Z/u)]$ contains D_s , d_p , u and the packed bed chromatography column length Z . The residence time based on u is defined as $t_r = Z/u$ in this study while the residence time based on u_0 , RT ($= Z/u_0 = V_t/F_v = t_r/\epsilon$) is more commonly used. u_0 ($= u\epsilon$) is the superficial velocity, ϵ is the void fraction of the packed bed column, and F_v is the volumetric flow rate.

2.2 | Linear flow velocity gradient

The concept of LFG is schematically shown in Figure 1. During the usual constant flow-velocity (CF) operation, the loaded amount of the sample protein M_{load} increases with time t linearly as shown in Figure 1a until it reaches the maximum amount allowed at the assigned flow velocity (or t_r), M_{col} , which can be calculated with DBC or V_B as a function of velocity u (or t_r):

$$M_{col} = DBC \cdot V_t = C_0 V_B \quad (3)$$

M_{load} is described by the following equation with the volumetric flow rate F_v .

$$M_{load} = \int_0^t C_0 F_v(t) dt \quad (4)$$

For LFG, $F_v(t)$ is described as a linear function of time t by

$$F_v = \frac{(F_{v2} - F_{v1})}{t_g} t + F_{v1} \quad (5)$$

F_{v1} and F_{v2} are the F_v values at the start and the end of LFG, respectively. t_g is the duration of the flow gradient. Equation (4) is then given by Equation (6) for LFG:

$$M_{load} = C_0 \left(F_{v1} t - \frac{(F_{v1} - F_{v2}) t^2}{2} \right) \quad (6)$$

As shown in Figure 1b, M_{load} does not increase linearly with t for LFG. M_{col} increases with t as u decreases with t (increase in t_r with t). Equation (7) must be fulfilled for LFG and also for CF. The curve a in Figure 1b is the optimum LFG whereas curve b results in the loss (leakage) from the column:

$$M_{load} \leq M_{col} \quad (7)$$

In addition to Equation (7), the proper gradient time t_g for LFG should be chosen according to the following equation:

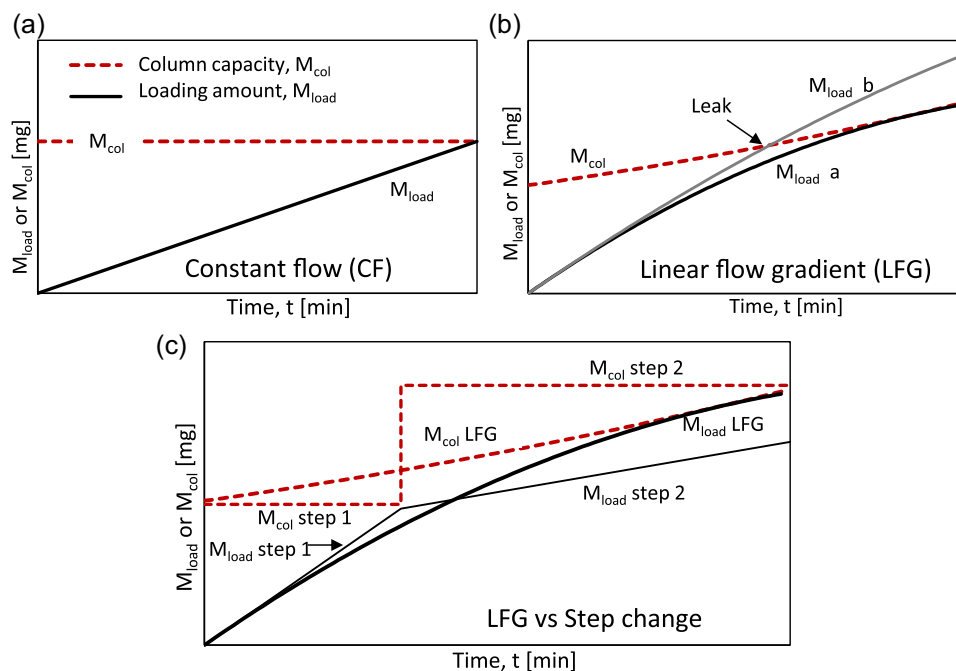


FIGURE 1 Loading amount M_{load} or column capacity M_{col} as a function of time t for constant-flow (CF) (a), linear flow-velocity gradient (LFG) (b), and step-change flow program (c) [Color figure can be viewed at wileyonlinelibrary.com]

$$\frac{DBC_1 V_t}{F_{v1} C_0} \leq t_g \leq \frac{DBC_2 V_t}{F_{v2} C_0}, \quad (8)$$

where DBC_1 and DBC_2 are the $DBC_{1\%}$ at F_{v1} and F_{v2} , respectively. The above equation is simply rewritten with the breakthrough time $t_B = V_B/F_v$ as

$$t_{B1} \leq t_g \leq t_{B2}, \quad (9)$$

where t_{B1} and t_{B2} are the breakthrough time at F_{v1} and F_{v2} , respectively. Namely, the resin utilization becomes higher when t_g is closer to t_{B2} , which is determined by DBC at $F_v = F_{v2}$, and may have better performance than step change under the premise that loading does not exceed capacity. The optimal t_g can be obtained by iterated calculations.

The comparison between the two-step-change flow-programming and LFG is shown in Figure 1c. By using less step changes for step-change flow programming, the design variables such as step duration and step flow rates can be reduced. On the other hand, multi-step changes can provide a better resin utilization. By transforming a multi-step to LFG, all the steps can be merged as a linear function. The design variables will not increase during process development with additional space for the process efficiency improvement.

3 | MATERIALS AND METHODS

3.1 | Materials

A 0.2 ml OPUS MiniChrom column (Repligen) packed with SP Sepharose Fast Flow (SPFF) (90 μ m; Cytiva) was used for breakthrough

experiments in cation exchange chromatography. The column was 1 cm long with 0.5 cm in inner diameter. Another 1 ml OPUS MiniChrom column packed with MabSelect SuRe (MSS) (85 μ m; Cytiva) with 2 cm in length and 0.8 cm in inner diameter was used for protein A chromatography.

Purified humanized IgG in clarified supernatants were used in the study, which were produced from Chinese hamster ovary cell fermentation. Buffer exchange by TFF using Pellicon XL Cassette of Ultracel-30 (MilliporeSigma) and dilution with corresponding adsorption buffers to 1 and 2.2 g/L of IgG for SPFF and MSS columns respectively were performed. Samples were stored at -80°C and thawed before usage. Samples were filtered using 0.45 μ m Millex-HV syringe PVDF membrane filter before injecting samples to columns. Chemicals for buffers were obtained from FUJIFILM Wako Pure Chemical (Osaka, Japan) in analytical grade.

3.2 | Breakthrough curve experiments

The breakthrough curve (BTC) experiments for SPFF were carried out using a PU-1580 pump (JASCO, Tokyo, Japan) connected to a UV detector UV-970 (JASCO) at $F_v = 0.035, 0.07, 0.142, 0.283,$ and 0.708 ml/min. The sample loading was stopped when $X = C/C_0$ reached 0.8. The equilibrium buffer was 10 mM citrate buffer (pH 5) containing 30 mM NaCl. The same buffer containing 1 M NaCl was used for elution (desorption). Flow programming was performed manually for stepwise change or by using the flow-rate program in the PU-1580 pump for LFG. The sample (IgG) concentration C_0 was 1 g/L.

The BTC experiments for MSS were performed at $F_v = 0.125, 0.25, 0.5,$ and 1 ml/min using ÄKTA Explorer (Cytiva). The binding (equilibrium) buffer and elution buffer were 20 mM sodium phosphate with 150 mM NaCl at pH 7.2 and 0.1 M sodium citrate at pH 3.5 , respectively. 2.2 g/L of IgG was used as the feed. LFG experiments were performed using ÄKTA Explorer with an additional injection valve bypassing the mixer. The flow path of buffer B was connected to the waste line to establish LFG.

The residence time based on the void volume was calculated as $t_{r1} = V_o/F_{v1}$ and $t_{r2} = V_o/F_{v2}$, where column void volume $V_o = \epsilon V_t$. It should be noted that although F_v is a linear function of time t , t_r is nonlinear with t in LFG.

3.3 | Flow programming in 4-column PCCC processes

LFG was applied to the loading in a 4-column PCCC process as shown in Figure S1 (supporting information). The cycles begin after start-up phase with time duration of t_1 , and is completed when all columns finished loading, post-load wash (PLW) and non-loading phase including elution, cleaning-in-place (CIP), and re-equilibration. Although continuous loading was assumed, LFG was not applied during the PLW phase as the time for PLW is relatively short compared to the total loading time in PCCC. Instead, F_{v2} was used for the loading during t_{PLW} .

Different $X\%$ of DBC was selected as the switching point for the first column by achieving the maximum loading in two connected (tandem) columns under the constraint of $X = 1\%$ in the outlet column (second column) throughout the operation when CF was used. Since the duration of PLW and non-loading steps had been decided, loading amount at each step can be calculated from the flow rate and the BTCs from experiments. By iterations, the $X\%$ at the switching point can be obtained. Productivity P was calculated by

$$P = \frac{F_v C_0}{n_{col} V_t}, \quad (10)$$

where n_{col} is the total number of columns.

LFG was designed for the tandem columns with the same constraint by Equation (7). The t_r in the PCCC was for the tandem columns.

4 | RESULTS

4.1 | Dynamic binding capacities from breakthrough curves

DBC_{1%} values obtained from experimental BTCs for both SPFF and MSS columns are shown in Figure 2. The DBC values obtained were similar as in other studies (Ghose et al., 2014; Hardin et al., 2009;

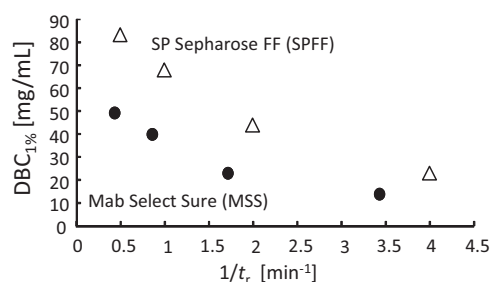


FIGURE 2 DBC_{1%} as a function of $1/t_r$ for SP Sepharose Fast Flow (SPFF) and MabSelect SuRe (MSS)

Ishihara et al., 2010). The DBC_{1%} was correlated with t_r by Equations (11) and (12) with $R^2 > 0.9$:

$$\text{SPFF: DBC}_{1\%} = 96.95e^{-0.373/t_r}, \quad (11)$$

$$\text{MSS: DBC}_{1\%} = 55.40e^{-0.425/t_r}. \quad (12)$$

DBC_{1%} can decrease linearly with $1/t_r$. The values at the shortest t_r deviated from the linear relationship. Those values were difficult to determine as the BTC curves were very broad and skewed. If we neglect those values, the data were well correlated by the linear relationship between E^* and F^* based on Equation (2).

Similar results including DBC_{1%} and DBC_{10%} for protein A resins were reported in previous studies (Angarita et al., 2015; Carta, 2012; Chen et al., 2020; Yoshimoto et al., 2016). Equations (11) and (12) were then used in Equation (7) to obtain LFG parameters (F_{v1} , F_{v2} , and t_g).

4.2 | Linear flow-velocity gradient

Flow programming experimental results for 1 g/L IgG with the SPFF column, including a 4-step change and LFG are shown in Figure 3a. M_{col} and M_{load} were calculated by Equations (3-6), (11) and (12). The BTCs by the 4-step change and LFG were similar to the BTC by CF ($t_{r2} = 1$ min). The BTC of LFG, which is similar to the BTC by CF ($F_v = F_{v2}$), will not start until M_{load} exceed M_{col} .

Similar results were obtained for MSS as shown in Figure 3b. t_{r1} was 0.3 min and t_{r2} was 1.2 min. M_{load} was estimated to be close to M_{col} during the interval of 10 – 15 ml in elution volume by calculation, and was reflected in a small bump in the breakthrough curve. Since the difference between M_{load} and M_{col} in LFG is not consistent as DBC was not linear during the gradient, the breakthrough will decrease when the capacity becomes much higher than the loading amount during flow programming. Similar effects can be seen in the manually controlled 4-step flow in Figure 3a.

By using DBC as a function of t_r , LFG (F_{v1} , F_{v2} , and t_g) can be designed to either shorten the loading time t_{load} or increase DBC. To show the advantage of LFG, DBC_{10%} values of IgG for SPFF were examined. DBC_{10%} rather than DBC_{1%} was selected for the visibility in the improvement.

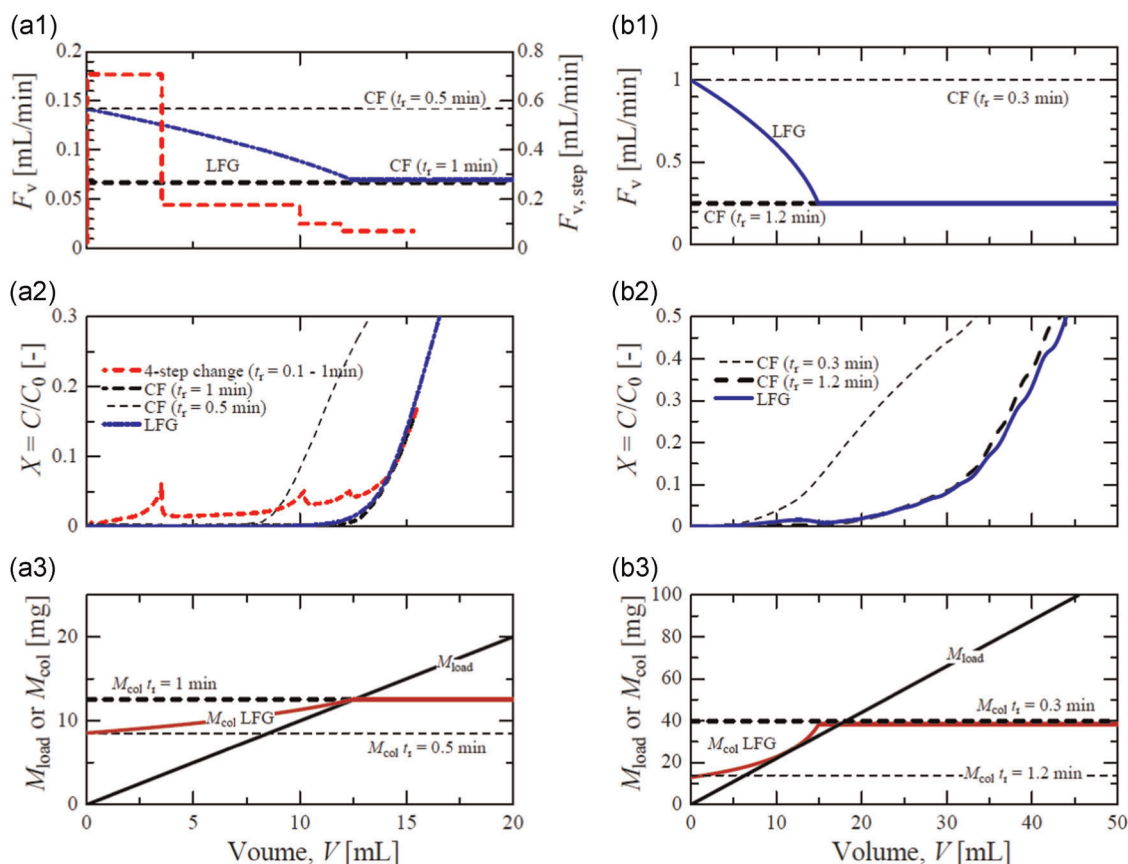


FIGURE 3 Comparison of flow rates, breakthrough curves, and loading amounts (from up to bottom) in (a) SP Sepharose Fast Flow (SPFF) at constant flow-velocity (CF) ($t_r = 0.5$ and 1.0 min), 4-step change ($t_{r1} = 0.1$, $t_{r2} = 0.4$, $t_{r3} = 0.7$, $t_{r4} = 1.0$ min) and linear flow-velocity gradient (LFG) with $(t_{r1}, t_{r2}) = (0.5, 1.0)$ min. The same comparison was shown in (b) MSS between CF at $t_r = 0.3$ and $t_r = 1.2$ min and LFG at $(t_{r1}, t_{r2}) = (0.3, 1.2)$ min. M_{col} for CF are shown in dashed lines. Elution volume in the x-axis is shared in (a1)–(a3) and (b1)–(b3) [Color figure can be viewed at wileyonlinelibrary.com]

The productivity P in LFG is calculated by Equation (13), using M_{load} or the volume of the sample loaded V_{load} and the gradient time t_g :

$$P = \frac{C_0 V_{load}}{V_t t_g} = \frac{M_{load}}{V_t t_g} = \frac{C_0 \int_0^{t_g} F_v dt}{V_t t_g} = \frac{C_0 (F_{v1} + F_{v2})}{2V_t} = \frac{C_0}{2} \left(\frac{1}{t_{r0.1}} + \frac{1}{t_{r0.2}} \right) \quad (13)$$

P is now independent of the gradient time t_g and only related to the sum of F_{v1} and F_{v2} or $1/t_{r0.1}$ and $1/t_{r0.2}$. When faster flow rate is applied, higher productivity can be achieved because of the shorter t_g . However, the loading amount M_{load} becomes smaller as DBC decreases with increasing F_v , as shown in Table S1 in supporting information. Under the same F_{v1} and F_{v2} , P remains constant and independent of the slope of the gradient.

As shown in Figure 4a, LFG ($t_r = 0.5$ to 2 min) reduced the loading time t_{load} by 56% while maintaining the same DBC (86 mg/ml) as that for CF ($t_r = 2.09$ min) shown in Figure 4b. This means that an approximately two-fold increase in P is possible by LFG.

4.3 | Application of LFG to continuous chromatography

Since LFG was shown to be effective for reducing the loading time, we attempted to apply LFG to the continuous capture process by a 4-column PCCC with the MSS columns.

Non-loading steps including 2 column volume (CV) of post-load-wash (PLW), 5 CV of elution, 15 min of CIP, and 5 CV of re-equilibrium with $t_r = 1$ min were used. Different LFG programs were examined in the range of $t_r = 0.3$ –2.4 min for their productivities and the holding time before breakthrough as displayed in Figure 5a,b. Each loading condition (t_g) was optimized to reach maximum capacity utilization with outlet breakthrough less than 1% of $X = C/C_0$. Considering the constraints in continuous chromatography, loading time should satisfy Equation (14), which was 13.5 min in the 4-column PCCC case discussed:

$$t_{load} = (t_{PLW} + t_g) \geq \frac{t_{non-load}}{n_{col} - 2}, \quad (14)$$

where t_{load} is the time for loading and $t_{non-load}$ is the total time to perform PLW, elution, CIP, and re-equilibration. The conditions and

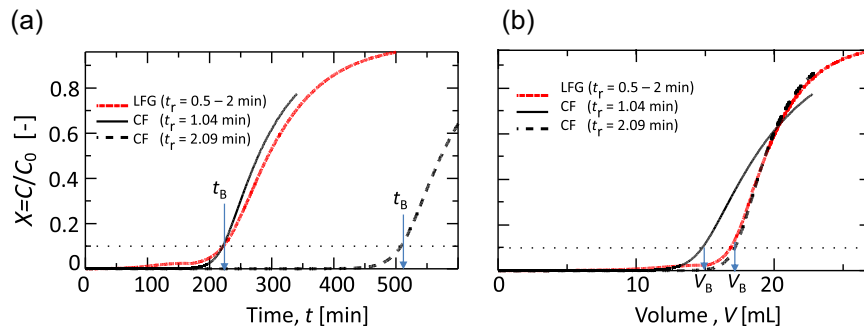


FIGURE 4 Process efficiency improvement by linear flow-velocity gradient (LFG) for SP Sepharose Fast Flow (SPFF) in the comparison of (a) X versus time t , and (b) X versus volume V . For $t_r = 1.04$ min, $RT = 2.89$ min, $DBC_{10\%} = 77$ mg/ml and $t_{B,10\%} = 222$ min. For $t_r = 2.09$ min, $RT = 5.81$ min, $DBC_{10\%} = 87$ mg/ml and $t_{B,10\%} = 508$ min. For $t_r = 0.5 - 2.0$ min (LFG), $RT = 1.4 - 5.6$ min, $DBC_{10\%} = 86$ mg/ml and $t_{B,10\%} = 222$ min [Color figure can be viewed at wileyonlinelibrary.com]

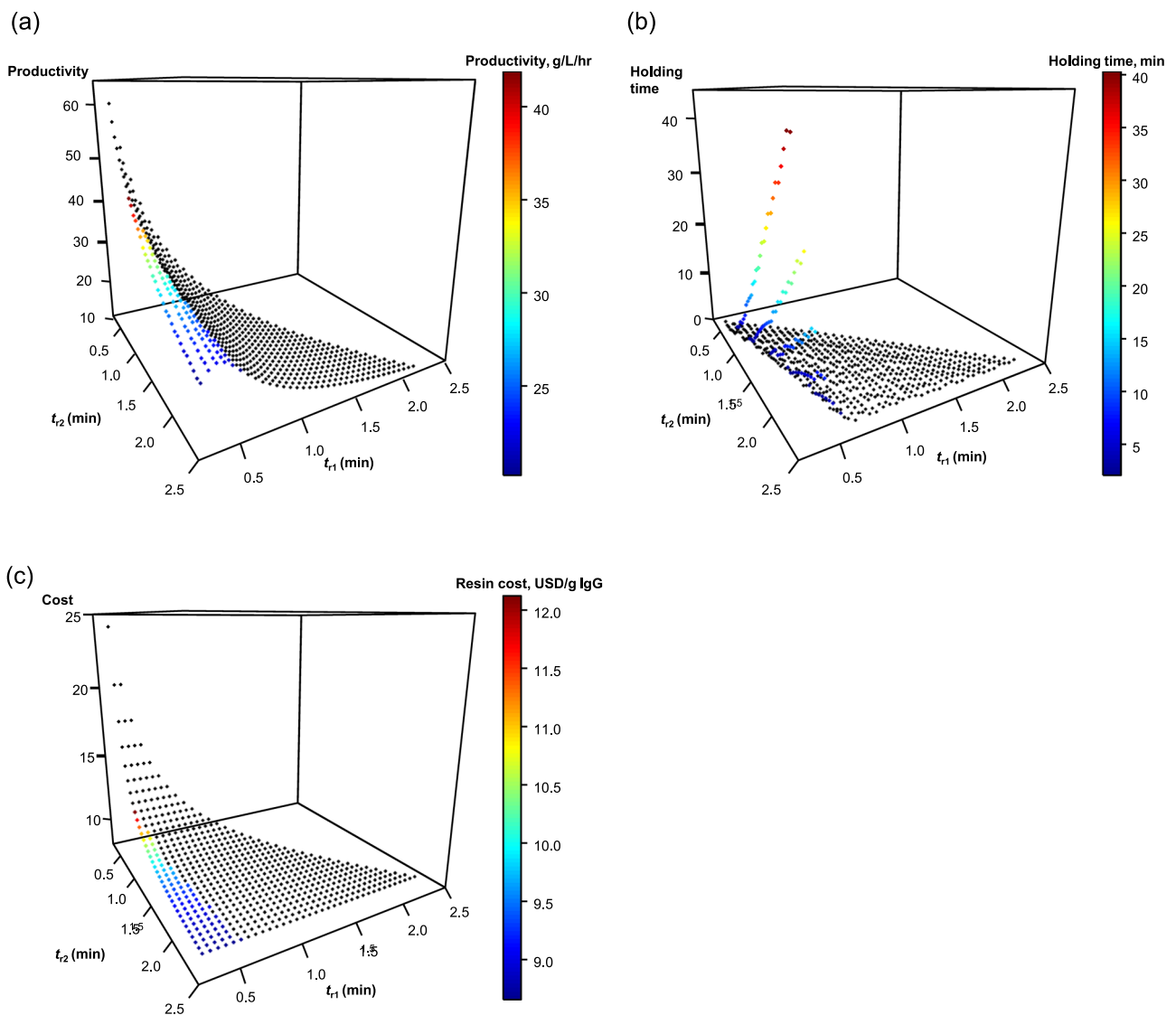


FIGURE 5 (a) Simulated productivity, (b) holding time between t_g and loading time, and (c) resin cost in the 4-column periodic counter-current chromatography (4C-PCCC) process. The conditions that satisfied PCCC constraints were labeled with colors while the scanning points between $t_r = 0.3$ and $t_r = 2.4$ min were labeled in black. (t_{r1}, t_{r2}) are x - and y -axis, respectively [Color figure can be viewed at wileyonlinelibrary.com]

	Constant flow (CF)				Linear flow-velocity gradient (LFG)		
	0.3	0.6	1.2	2.4	0.3–0.8	0.3–1.2 ^b	0.4–2.3
Residence time, t_r (min)	0.3	0.6	1.2	2.4	0.3–0.8	0.3–1.2 ^b	0.4–2.3
Loading time per column (min)	23.9	72.8	154.1	338.9	23.6	34.2	60.8
Gradient time, t_g (min) ^c	–	–	–	–	20.4	23.9	45.5
Productivity, P (g/L/h)	33.0	16.5	8.3	4.1	41.9	33.8	22.8
Resin cost (USD/g IgG) ^d	15.2	10.0	9.4	8.6	12.1	10.4	8.7

^a1 ml MabSelect SuRe column was used with 2.2 g/L of IgG as feed.

^bCondition which has the lowest resin cost with higher productivity compared to CF ($t_r = .3$ min).

^cLFG for the highest productivity and the lowest resin cost are shown.

^dPer 50 cycles with resin cost of 10,000 USD/L resin.

TABLE 1 Loading conditions and process performances in a 4-column PCCC process^a

performances satisfied the PCCC constraints are listed in Table S2 in supporting information.

Table 1 shows the performance comparison between CF and LFG. In the case of CF, compared to $t_r = 0.6$ min (reference), loading at $t_r = 0.3$ min helped double the productivity by reducing 60% of the loading time. At short t_r values although the DBC became lower, the reduction in t_{load} was more significant for increasing the productivity. Similar results can be found in other PCCC studies with RT comparison (Baur et al., 2016; Godawat et al., 2012). By replacing CF with LFG, P was further increased. In the case of LFG ($t_r = 0.3 - 0.8$ min), P was increased to 2.5 times with 67% reduction in loading time compared to CF at $t_r = 0.6$ min. Using the design methodology for LFG proposed in the study, LFG achieved the maximum $t_{load} = 20.4$ min without leakage, and had 3 min of holding time before reaching $X = 1\%$ after t_{load} , which satisfied Equation (14). LFG ($t_r = 0.3 - 1.2$ min) adopted the same loading time as CF at $t_r = .3$ min. Although t_{load} for LFG was longer due to the holding time, P was almost the same as that at $t_r = 0.3$ min. In the case of a longer gradient ($t_r = 0.4 - 2.3$ min, $t_g = 45.5$ min), 15.3 min of holding time at F_{v2} was required to reach DBC_{1%} after t_g and made $t_{load} = 60.8$ min. While loading capacity was increased to almost double in $t_r = 0.4 - 2.3$ min compared to $t_r = 0.6$ min based on the DBC - t_r correlation, productivity had 1.4 times increase, which was lower than $t_r = 0.3 - 0.8$ min because of the longer loading time. Although it is possible to design a gradient in LFG from $t_r = 0.3$ to $t_r < 0.8$ min, the loading time will not match the constraints in PCCC and thus fail to deliver a continuous loading. As a result, the optimal LFG was found to be $t_r = 0.3 - 0.8$ min if the goal is to achieve maximum productivity.

All three LFG cases showed higher P values compared to CF at $t_r = 0.6$ min due to the shorter loading time. As demonstrated in Table 1, P can be increased without sacrificing the loading time as long as extra holding time before reaching the Mcol can satisfy the PLW step. Compared to a gradient ending at high RT with high capacity, an optimal gradient ending at lower t_r without redundant holding time can boost productivity to a higher number by increasing capacity in a shorter gradient (Figure 5b). Although P was reduced to half in the case of CF ($t_r = 0.6$ min) compared to CF ($t_r = 0.3$ min), the decrease in P was less sensitive to F_{v2} between LFG ($t_r = 0.3 - 0.8$ min) and LFG ($t_r = 0.3 - 1.2$ min). P for LFG can remain relatively stable

regarding to the variations in F_v compared to CF, where similar results were observed in the statistical models of tri-step flow rate in another study for batch chromatography (Bjorkman, 2014).

The resin cost evaluation by LFG was examined as the high cost in Protein A resin (5500–16000 USD/L) is one of the challenging problems in the downstream of mAb products (Franzreb et al., 2014; Bracewell et al., 2015; Tosoh, n.d.). Re-use of Protein A resins has been studied by many researchers, and the factors that can influence the lifetime of protein A resin include the residual of impurities such as HCP, lipid, and nucleic acid after CIP, and the hydrolysis of protein A ligand during CIP (Jiang et al., 2009; Bracewell et al., 2015). With more purification cycles performed, the degradation in the ligand may result in lower binding capacities. LFG can be an alternative to extend the resin lifetime by processing more mAb in the same number of the purification cycle. As the performance in purity and yield of mAb by MSS has been shown to be nearly consistent without loss within 50 cycles of purification process (Hahn et al., 2006; Lintern et al., 2016; Zhang et al., 2017), a cost comparison of CF with LFG was conducted as shown in Table 1 and Figure 5c. The changes in cost were calculated according to the cost of resin per the amount of mAb being processed after 50 cycles for both CF and LFG cases.

Different from the productivity, the cost of resin per unit amount of mAb processed after 50 cycles increased when higher flow rates were applied due to the decreased amount in loading as shown in the comparison between CF ($t_r = 0.3$ min) and CF ($t_r = 0.6$ min). Similar results were obtained for LFG. Namely, the cost increased with decreasing t_{load} . The cost for LFG ($t_r = 0.3 - 1.2$ min) was nearly 30% lower than that for CF ($t_r = 0.3$ min) although P values were similar.

As there is leverage between resin cost per amount of mAb processed and productivity, it becomes necessary to consider not just the productivity but also capacity utilization when choosing the optimized condition for LFG. Of course, the impact from both productivity and capacity utilization to the overall cost of goods should be considered carefully as the resin (consumable) cost decreases, the lower productivity can affect the overall cost per unit product produced (Franzreb et al., 2014; Thillaiyinayagalingam et al., 2012). However, the results confirmed that a better balance between productivity and resin cost can be achieved by adopting LFG compared to CF for the loading.

5 | DISCUSSION

Various parameters such as composition, temperature, pressure and flow can be used as a programmed parameter of chromatography. For liquid chromatography (LC) of proteins and other biologics, composition (mobile phase modifier) is the most commonly employed parameter for the elution. For example, the linear increase in the salt concentration known as linear gradient elution (LGE) is widely used for ion-exchange chromatography (IEC) of proteins. Temperature and pressure are not used as the programmed parameter for process chromatography of proteins.

Flow (velocity) is another parameter that can control the chromatographic separation performance. However, it has not been extensively studied for LC. Flow-velocity programming (flow-gradient) experiments (from low to high velocity) were carried out with monolithic columns to reduce the separation time (Cabo-Calvet et al., 2014; Nesterenko & Rybalko, 2004). Higher flow-velocities were possible because the column performance of monolithic columns does not depend on the flow-velocity.

Flow-programming from high to low flow velocities can be employed to increase the capture process efficiency of proteins. This method is possible because of the zone self-sharpening effect, by which a partially broadened zone in the column at the high velocity can be compressed again with the lower velocity. This mechanism can be explained by the zone self-sharpening effect in the column (see Appendix A). The effect exists due to the moving velocity of the protein governed by the concentration. Because of this effect, a partially broadened zone in the column at the high velocity can be compressed again with the lower velocity. This effect is more pronounced when the isotherm is "favorable." It is known that isotherms of mAb for protein A chromatography or ion-exchange chromatography are highly favorable. For the linear isotherm, LFG does not work as the zone self-sharpening effect does not exist.

For process chromatography, often LGE processes are converted to stepwise elution processes mainly because LGE processes need a special skid for making a linear salt or pH gradient with time. A special device is not needed for LFG provided that the pump flow rate can be programmed.

In the present works, the empirical relationship between DBC and t_r was used in designing the LFG. This method is robust and more practical as compared to the mechanistic models and DoE methods-based approaches. The relationship can be generalized by using $E^* = \text{DBC}/\text{SBC}$ and a dimensionless group F^* including particle size, pore diffusion coefficient, and RT for the application in different media and biomolecules (Chen et al., 2020). It has been reported that for protein A chromatography columns the ratio of DBC/SBC is independent of the feed concentration for a rectangular isotherm with mass transfer dominated by pore diffusion, and the DBC can be estimated by RT without prior knowledge of mass transfer (Carta, 2012; Chen et al., 2020; Pabst et al., 2018). By adopting the relationship and

merging step-change to LFG, the number of design variables and computation power required can be reduced while the robustness of the process performance in productivity is still maintained. The increase in capacity utilization can also extend the resin lifetime by having less cycles of CIP per amount of mAb being processed and reduce the consumable cost in consequence.

However, it should be noted that the maximum productivity condition is not the most economical condition as many other factors such as buffer costs, energy consumptions and equipment footprints must be considered. A thorough techno-economic analysis may be needed when evaluating the overall cost of goods per batch of mAb produced.

6 | CONCLUSIONS

A new method for increasing the capture chromatography process efficiency, LFG was proposed, and verified experimentally by ion-exchange chromatography (SPFF) and protein A chromatography (MSS) of mAb.

The method uses the total column capacity M_{col} and the total loaded amount M_{load} as a function of time, t . M_{col} can be calculated by using the relationships between $\text{DBC}_{1\%}$ and t_r . M_{load} is calculated by the LFG time t_g , the starting flow rate F_{v1} and the final flow rate F_{v2} . By considering M_{load} and M_{col} , and the required conditions, the optimum LFG can be designed. The method was verified by experimental data. The loading time t_{load} by LFG decreased by a factor of ca. 2.0 compared with t_{load} for the CF. The process efficiency improvement is more pronounced when the isotherm is highly favorable and the loading volume is large.

The case study in a 4-column PCCC process with MSS also demonstrated the reduction in process time and the increase in productivity using LFG compared to the conventional CF loading. Even when lower F_{v2} is applied, total productivity becomes less prone to the changes in flow rates as the duration in loading time can be reduced compared to CF because of the continuous increase in DBC during LFG.

By adopting the relationship and merging step-change to LFG, the number of design variables and computation power required can be reduced while the robustness of the process performance in productivity is still maintained. The increase in M_{load} can also extend the resin lifetime by having less cycles of CIP per amount of mAb being processed and reduce the consumable cost in consequence, while the overall cost of goods per mAb produced needs to be evaluated by considering the other downstream unit operations.

ACKNOWLEDGMENT

This study was partially supported by AMED under Grant Number JP18ae0101056, JP19ae0101056, and JP20ae0101056.

CONFLICT OF INTERESTS

The authors declare that there are no conflict of interests.

AUTHOR CONTRIBUTIONS

Chyi-Shin Chen and Kosei Ando performed experiments according to the original idea by Shuichi Yamamoto, Chyi-Shin Chen, Noriko Yoshimoto, and Shuichi Yamamoto discussed the results and a calculation method developed in this study. Chyi-Shin Chen and Shuichi Yamamoto wrote the paper based on discussion with Noriko Yoshimoto.

ORCID

Chyi-Shin Chen  <https://orcid.org/0000-0003-3971-9963>

Noriko Yoshimoto  <https://orcid.org/0000-0002-3171-9953>

Shuichi Yamamoto  <http://orcid.org/0000-0002-6756-9141>

REFERENCES

- Angarita, M., Müller-Spáth, T., Baur, D., Lievrouw, R., Lissens, G., & Morbidelli, M. (2015). Twin-column capture SMB: A novel cyclic process for protein A affinity chromatography. *Journal of Chromatography A*, 1389, 85–95. <https://doi.org/10.1016/j.chroma.2015.02.046>
- Baur, D., Angarita, M., Müller-Spáth, T., Steinebach, F., & Morbidelli, M. (2016). Comparison of batch and continuous multi-column protein A capture processes by optimal design. *Biotechnology Journal*, 11, 920–931. <https://doi.org/10.1002/biot.201500481>
- Becerra-Arteaga, A. (2016). Simple process strategies to increase the utilization of protein A media in clinical manufacturing. Paper presented at 251st ACS National Meeting, BIOT 390, San Diego.
- Bjorkman, T. (2014). Optimizing productivity on high capacity Protein A affinity resin. Paper presented at 247th ACS National Meeting, BIOT 393, Dallas.
- Bracewell, D. G., Pathak, M., Ma, G., & Rathore, A. S. (2015). Re-use of protein A resin: fouling and economics. *BioPharm International*, 28(3), 28–33. <https://www.biopharminternational.com/view/re-use-protein-resin-fouling-and-economics>
- Cabo-Calvet, E., Ortiz-Bolsico, C., Baeza-Baeza, J., & García-Alvarez-Coque, M. (2014). Description of the retention and peak profile for chromatolith columns in isocratic and gradient elution using mobile phase composition and flow rate as factors. *Chromatography*, 1, 194–210. <https://doi.org/10.3390/chromatography1040194>
- Carta, G. (2012). Predicting protein dynamic binding capacity from batch adsorption tests. *Biotechnology Journal*, 7, 1216–1220. <https://doi.org/10.1002/biot.201200136>
- Carta, G., & Jungbauer, A. (2010). *Protein chromatography: Process development and scale-up*, New York: John Wiley & Sons.
- Chen, C.-S., Yoshimoto, N., Yamamoto, S., & S. (2020). Prediction of the performance of capture chromatography processes of proteins and its application to the repeated cyclic operation optimization. *Journal of Chemical Engineering of Japan*, 53, 689–697. <https://doi.org/10.1252/jcej.20we116>
- Ecker, D., Jones, S. D. M., & Levine, H. L. (2015). The therapeutic monoclonal antibody market. *mAbs*, 7, 9–14.
- Fahrner, R. L., Iyer, H. V., & Blank, G. S. (1999). The optimal flow rate and column length for maximum production rate of protein A affinity chromatography. *Bioprocess Engineering*, 21, 287–292. <https://doi.org/10.1007/s004490050677>
- Franzreb, M., Müller, E., & Vajda, J. (2014). Cost estimation for protein A chromatography: An in silico approach to Mab purification strategy. *BioProcess International*, 12, 44–52.
- Ghose, S., Nagrath, D., Hubbard, B., Brooks, C., & Cramer, S. M. (2004). Use and optimization of a dual-flowrate loading strategy to maximize throughput in protein-A affinity chromatography. *Biotechnology Progress*, 20, 830–840. <https://doi.org/10.1021/bp0342654>
- Ghose, S., Zhang, J., Conley, L., Caple, R., Williams, K. P., & Cecchini, D. (2014). Maximizing binding capacity for protein A chromatography. *Biotechnology Progress*, 30, 1335–1340. <https://doi.org/10.1002/btpr.1980>
- Godawat, R., Brower, K., Jain, S., Konstantinov, K., Riske, F., & Warikoo, V. (2012). Periodic counter-current chromatography—Design and operational considerations for integrated and continuous purification of proteins. *Biotechnology Journal*, 7, 1496–1508. <https://doi.org/10.1002/biot.201200068>
- Hahn, R., Shimahara, K., Steindl, F., & Jungbauer, A. (2006). Comparison of protein A affinity sorbents III. Life time study. *Journal of Chromatography A*, 1102, 224–231.
- Hardin, A. M., Harinarayan, C., Malmquist, G., Axén, A., & van Reis, R. (2009). Ion exchange chromatography of monoclonal antibodies: Effect of resin ligand density on dynamic binding capacity. *Journal of Chromatography A*, 1216, 4366–4371.
- Ishihara, T., Nakajima, N., & Kadoya, T. (2010). Evaluation of new affinity chromatography resins for polyclonal, oligoclonal and monoclonal antibody pharmaceuticals. *Journal of Chromatography B*, 878, 2141–2144.
- Jiang, C., Liu, J., Rubacha, M., & Shukla, A. A. (2009). A mechanistic study of Protein A chromatography resin lifetime. *Journal of Chromatography A*, 1216, 5849–5855.
- LeVan, M. D., Carta, G., & Yon, C. M. (1997). Section 16: Adsorption and ion exchange. In R. H. Perry, D. W. Green, & J. O. Maloney (Eds.), *Perry's Chemical Engineers, Handbook* (7th ed.). New York: McGraw-Hill.
- Lintern, K., Pathak, M., Smales, C. M., Howland, K., Rathore, A., & Bracewell, D. G. (2016). Residual on column host cell protein analysis during lifetime studies of protein A chromatography. *Journal of Chromatography A*, 1461, 70–77.
- Nesterenko, P. N., & Rybalko, M. A. (2004). The use of a continuous flow gradient for the separation of inorganic anions on a monolithic disk. *Mendeleev Communications*, 14, 121–122. <https://doi.org/10.1070/MC2004v014n03ABEH001914>
- Pabst, T. M., Thai, J., & Hunter, A. K. (2018). Evaluation of recent Protein A stationary phase innovations for capture of biotherapeutics. *Journal of Chromatography A*, 1554, 45–60.
- Sellberg, A., Nolin, M., Löfgren, A., Andersson, N., & Nilsson, B. (2018). Multi-flowrate optimization of the loading phase of a preparative chromatographic separation. *Computer Aided Chemical Engineering*, 43, 1619–1624.
- Shukla, A. A., Wolfe, L. S., Mostafa, S. S., & Norman, C. (2017). Evolving trends in mAb production processes. *Bioengineering & Translational Medicine*, 2, 58–69. <https://doi.org/10.1002/btm2.10061>
- Thillaivinayagalingam, P., Reidy, K., Lindeberg, A., & Newcombe, A. R. (2012). Revisiting protein A chromatography. *BioProcess International*, 10(3).
- Tosoh (n.d.). A high capacity protein A resin designed to reduce production costs. <https://www.separations.eu.tosohbioscience.com/FileLibrary/TBG/ProductsDownload/ApplicationNote/a16p04a.pdf>
- Woodcock, J. (2014). Modernizing pharmaceutical manufacturing—continuous manufacturing as a key enabler. International Symposium on Continuous Manufacturing of Pharmaceuticals, Cambridge, MA. https://iscmp2014.mit.edu/sites/default/files/documents/ISCMP2014_Keynote_Slides.pdf
- Yamamoto, S., Nakanishi, K., & Matsuno, R. (1988). *Ion-exchange chromatography of proteins*, Boca Raton: CRC.
- Yoshimoto, N., Yada, T., & Yamamoto, S. (2016). A Simple method for predicting the adsorption performance of capture chromatography of proteins. *Japan Journal of Food Engineering*, 17, 95–98. <https://doi.org/10.11301/jsfe.17.95>
- Yoshimoto, N., & Yamamoto, S. (2017). Simplified methods based on mechanistic models for understanding and designing chromatography processes for proteins and other biological products—Yamamoto Models and Yamamoto Approach. In A. Staby, A. S. Rathore, &

S. Ahuja (Eds.), *Preparative chromatography for separation of proteins* (pp. 111–157). Wiley. Chapter 4.

Zhang, J., Siva, S., Caple, R., Ghose, S., & Gronke, R. (2017). Maximizing the functional lifetime of Protein A resins. *Biotechnology Progress*, 33, 708–715.

SUPPORTING INFORMATION

Additional supporting information may be found online in the Supporting Information section.

How to cite this article: Chen C-S, Ando K, Yoshimoto N, Yamamoto S. Linear flow-velocity gradient chromatography—An efficient method for increasing the process efficiency of batch and continuous capture chromatography of proteins. *Biotechnology and Bioengineering*. 2021;118:1262–1272. <https://doi.org/10.1002/bit.27649>

APPENDIX A: SELF-SHARPENING EFFECT OF BREAKTHROUGH CURVES DURING FLOW-VELOCITY PROGRAMMED LOADING

To confirm the self-sharpening effect of breakthrough curves (BTCs) during the flow-velocity programmed loading, we calculated BTCs numerically based on the following mechanistic model, which includes the effective mass transfer coefficient, K_s . This model has been widely employed for analyzing BTCs for adsorption processes (Carta & Jungbauer, 2010; LeVan et al., 1997; Yamamoto et al., 1988; Yoshimoto & Yamamoto, 2017).

The equation for the mobile phase neglecting the axial dispersion is given by

$$\frac{\partial C}{\partial t^*} + H \frac{\partial \bar{C}_s}{\partial t^*} = -\frac{\partial C}{\partial z^*}. \quad (\text{A1})$$

Here, C is the mobile phase concentration. \bar{C}_s is the average stationary phase concentration. $H = (1 - \varepsilon)/\varepsilon$ is the volumetric phase ratio (ε : void fraction). $t^* = t/(Z/u)$ is the dimensionless time and $z^* = z/Z$ is the dimensionless distance from the column inlet. Z is the column length. The mobile phase velocity u is related to the volumetric flow-rate F_v and the column diameter d_c as $u = F_v/(\pi d_c^2 \varepsilon/4)$.

The linear driving force (LDF) equation for the stationary phase is given by

$$\frac{\partial \bar{C}_s}{\partial t^*} = K_s^*(KC - \bar{C}_s). \quad (\text{A2})$$

$K_s^* = K_s(Z/u)$ is the dimensionless mass transfer coefficient, which is the product of K_s and $t_r = Z/u$. $K = C_s/C$ is the distribution coefficient. The effective overall mass transfer coefficient K_s is related to the stationary phase diffusion coefficient D_s and the particle diameter d_p :

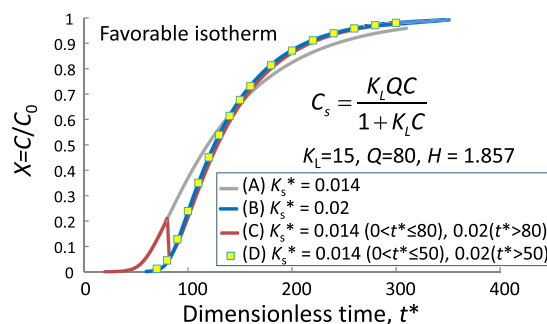


FIGURE A1 Numerically calculated breakthrough curves for the constant and the flow-programmed velocities for the favorable isotherm described by the Langmuir isotherm. $K_s^* = K_s (Z/u)$. The velocity u_2 for breakthrough curves (BTCs) (C) and (D) is $0.7 \times u$ for BTC (A). The sample feed concentration $C_0 = 1$ in this calculation

$$K_s = 60 D_s/d_p^2. \quad (\text{A3})$$

$K_0 = C_{s0}/C_0$ is the distribution coefficient for $C = C_0$. K was calculated by the Langmuir adsorption isotherm:

$$C_s = K_L QC / (1 + K_L C) = KC, \quad (\text{A4})$$

K is given by

$$K = K_L Q / (1 + K_L C). \quad (\text{A5})$$

$$\text{Then, } K_0 = K_L Q / (1 + K_L C_0). \quad (\text{A6})$$

Equations (A1) and (A2) were solved numerically with Equation (A4).

Figure A1 shows calculated BTCs for (A) the constant high flow velocity at $u = u_1$, (B) the constant low flow velocity at $u = u_2$, (C) the flow programming from $u = u_1$ to u_2 (u_2 at $t^* > 80$), and (D) the flow programming from $u = u_1$ to u_2 (u_2 at $t^* > 50$). When we look at BTC (C), the concentration X drops very sharply at $t^* = 80$ when the flow velocity is decreased to u_2 . After that, the BTC (C) is superimposed on BTC (B). This behavior was experimentally confirmed as shown in Results (Figure 3). Another flow-velocity programmed BTC (D) is

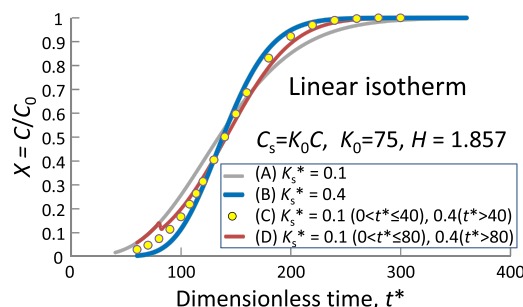


FIGURE A2 Numerically calculated breakthrough curves for the constant and the flow-programmed velocities for the linear isotherm. The velocity u_2 for breakthrough curves (BTCs) (C) and (D) is $0.25 \times u$ for BTC (A)

hardly distinguishable with BTC (B). As $u_1/u_2 = 1.43$, the breakthrough time t_b at $X = 0.1$ becomes shorter for BTC (D) by ca. 15%. This behavior is due to the favorable isotherm used in the calculation (large $K_L C_0$ values). The zone self-sharpening effect in the column exists due to the moving velocity of the protein governed by the concentration. Because of this effect, a partially broadened zone in

the column at the high velocity can be compressed again with the lower velocity. The constant-pattern curve is also due to this effect.

The zone self-sharpening effect does not exist for the linear isotherm. Eventually, DBC cannot be improved by using the flow-programming as shown in Figure A2. In this case DBC for the flow-programming becomes lower than that for the constant flow.